THE UNIVERSITY of EDINBURGH

Edinburgh Research Explorer

Inhibition of Ras/Erk1/2 signaling protects against post-ischemic renal injury.

Citation for published version:
Sabbatini, M, Santillo, M, Pisani, A, Paternò, R, Uccello, F, Serù, R, Matrone, G, Spagnuolo, G, Andreucci, M, Serio, V, Esposito, P, Cianciaruso, B, Fuiano, G & Avvedimento, EV 2006, 'Inhibition of Ras/Erk1/2 signaling protects against post-ischemic renal injury.', *American Journal of Physiology - Renal Physiology*, vol. 6, no. 290, pp. 1408-15. https://doi.org/10.1152/ajprenal.00304.2005

Digital Object Identifier (DOI):
10.1152/ajprenal.00304.2005

Link:
Link to publication record in Edinburgh Research Explorer

Document Version:
Publisher's PDF, also known as Version of record

Published In:
American Journal of Physiology - Renal Physiology

General rights
Copyright for the publications made accessible via the Edinburgh Research Explorer is retained by the author(s) and / or other copyright owners and it is a condition of accessing these publications that users recognise and abide by the legal requirements associated with these rights.

Take down policy
The University of Edinburgh has made every reasonable effort to ensure that Edinburgh Research Explorer content complies with UK legislation. If you believe that the public display of this file breaches copyright please contact openaccess@ed.ac.uk providing details, and we will remove access to the work immediately and investigate your claim.

OPEN ACCESS

Download date: 17. May. 2022

Am J Physiol Renal Physiol 290: F1408–F1415, 2006.
First published January 24, 2006; doi:10.1152/ajprenal.00304.2005.

Inhibition of Ras/ERK1/2 signaling protects against postischemic renal injury

Massimo Sabbatini,[1]* Mariarosaria Santillo,[2]* Antonio Pisani,[1] Roberto Paternò,[3] Francesco Uccello,[1] Rosalba Serù,[2] Gianfranco Matrone,[2] Gianrico Spagnuolo,[4] Michele Andreucci,[5] Vittorio Serio,[1] Pasquale Esposito,[1] Bruno Cianciaruso,[1] Giorgio Fuiano,[5] and Enrico V. Avvedimento[6]

[1]*Chair of Nephrology,* [2]*Department of Neuroscience, Unit of Physiology,* [3]*Department of Clinical and Experimental Medicine,* [4]*Department of Oral and Maxillofacial Sciences,* [5]*Chair of Nephrology, University Magna Graecia of Catanzaro, and* [6]*Department of Biology and Cellular and Molecular Pathology, University Federico II of Naples, Naples, Italy*

Submitted 28 July 2005; accepted in final form 18 January 2006

Sabbatini, Massimo, Mariarosaria Santillo, Antonio Pisani, Roberto Paternò, Francesco Uccello, Rosalba Serù, Gianfranco Matrone, Gianrico Spagnuolo, Michele Andreucci, Vittorio Serio, Pasquale Esposito, Bruno Cianciaruso, Giorgio Fuiano, and Enrico V. Avvedimento. Inhibition of Ras/ERK1/2 signaling protects against postischemic renal injury. *Am J Physiol Renal Physiol* 290: F1408–F1415, 2006. First published January 24, 2006; doi:10.1152/ajprenal.00304.2005.—The small GTPase p21 Ras and its downstream effectors play a central role in the control of cell survival and apoptosis. We studied the effects of Ras/ERK1/2 signaling inhibition on oxidative damage in cultured renal and endothelial cells and on renal ischemia-reperfusion injury in the rat. Primary human renal tubular and human endothelial ECV304 cells underwent significant cell death when subjected to oxidative stress. This type of stress induced robustly ERK1/2 and phosphoinositide 3-kinase (PI3-kinase) signaling. Inhibition of Ras/ERK1/2 with a farnesyl transferase inhibitor, chaetomellic acid A (S-FTI), or with PD-98059, an inhibitor of MEK, a kinase upstream ERK1/2, significantly reduced the fraction of dead cells. The inhibitor of the PI3-kinase/Akt pathway, LY-294002, failed to exert a protective effect. We have translated these data in a rat model of renal ischemic injury in vivo. In uninephrectomized animals, anesthetized with pentobarbital sodium (Nembutal, 50 mg/kg ip), 24 h after an acute ischemic renal insult (45-min occlusion of left renal artery) a significant fraction of kidney cells succumbed to cell death resulting in renal failure [glomerular filtration rate (GFR) 0.17 ± 0.1 vs. 0.90 ± 0.4 ml·min^{-1}·100 g body wt^{-1} in normal rats]. Rats treated with S-FTI maintained the renal function (GFR 0.50 ± 0.1 ml·min^{-1}·100 g body wt^{-1}), and the kidneys showed a significant reduction of tubular necrosis. Reduction of ischemic damage in kidney and tubular cells paralleled Ha-Ras inhibition, assayed by cytosolic translocation of the protein. These data demonstrate that inhibition of farnesylation and consequently of Ras/ERK1/2 signaling significantly reduces acute postischemic renal injury.

signal transduction; kidney; endothelium; farnesyl transferase inhibitors

ISCHEMIA-REPERFUSION INJURY (IRI) represents the first cause of acute renal failure in both native (24) and transplanted kidneys (7). IRI is an invariable occurrence in the transplanted kidney and significantly affects the outcome of the graft. It is known that a prolonged ischemia is a common cause of delayed graft function in renal-transplanted patients and represents a risk factor for both acute rejection (12) and chronic allograft nephropathy (16).

IRI is a complex sequence of events that involves a rise in reactive oxygen species (ROS) and synthesis of cytokines and chemokines, leading to inflammation and, eventually, to cell death (4, 17). Many experimental models have been developed in an attempt to prevent or limit renal failure after IRI, like the use of ROS scavengers (6, 17, 19) or of various drugs (10, 24, 25) or the induction of "renoprotective" genes (15) with disappointing and inconclusive results, which have not produced information on the molecular nature of the process and have been difficult to translate to human studies.

The elucidation of molecular pathways involved in tubular cell death following IRI can lead to the identification of potential targets for possible therapeutic intervention. One such target may be the small GTPase p21 Ras, which plays a central role in the signaling pathway controlling cell survival and apoptosis through its activation or inhibition in response to several stimuli. Oxidative stress is a powerful activator of Ras, and such activity is necessary for the transmission of signals by many cytokines involved in the ischemic insult, like PAF, transforming growth factor-β, and endothelin-1, to its downstream effectors, such as extracellular signal-regulated kinase (ERK) 1/2 and phosphoinositide 3-kinase (PI3-kinase), which are relevant stress responders (14). Recent studies in our laboratory have shown that two different isoforms of Ras, namely, Ha-Ras and Ki-Ras, act differently in response to an oxidative stimulus: the activation of Ha-Ras, in fact, increases the number of cells undergoing cell death by increasing intracellular ROS, whereas activation of Ki-Ras seems to have a protective effect through ROS reduction (3, 20). These findings highlight the modulatory role of Ras isoforms in response to oxidative injuries and suggest a crucial role of Ras as a preferential molecular target in disorders associated with high intracellular levels of ROS.

To date, however, no study has evaluated the function of Ras in renal damage after ischemia and the possibility to influence Ras activation in an attempt to mitigate renal injury.

The purpose of this study was to evaluate the signaling pathways involved in oxidative stress-induced cell damage in cultured human renal tubular cells and to test in vivo the protective role of Ras inhibition in an established model of warm IRI.

Ras association with the plasma membrane is essential for its biological activity. Proper membrane association is allowed by

*M. Sabbatini and M. Santillo contributed equally to this study.

Address for reprint requests and other correspondence: M. Santillo, Dept. of Neuroscience, Unit of Physiology, Univ. "Federico II" of Naples, Via S. Pansini, 5 80131 Naples, Italy (e-mail: marsanti@unina.it) or M. Sabbatini, Via A. Manzoni 50, 80123 Naples, Italy (e-mail: sabbatin@unina.it).

The costs of publication of this article were defrayed in part by the payment of page charges. The article must therefore be hereby marked "*advertisement*" in accordance with 18 U.S.C. Section 1734 solely to indicate this fact.

0363-6127/06 $8.00 Copyright © 2006 the American Physiological Society

Downloaded from journals.physiology.org/journal/ajprenal (092.021.147.200) on April 1, 2022.

a series of posttranslational modifications of the protein. The first consists of the covalent binding of a polyisoprenoid, a farnesyl group to the cysteine residue located in the COOH-terminal tetrapeptide (CAAX box), in a reaction catalyzed by farnesyl protein transferase (FPTase) (13). Therefore, several inhibitors of FPTase have been developed to inhibit Ras and its downstream effectors and some of them are currently used in clinical trials for cancer treatment (21). In our study, we inhibited Ras using a specific inhibitor of Ras farnesylation, chaetomellic acid A (S-FTI).

We have previously reported that endothelial cells treated with farnesyl transferase inhibitors or expressing a dominant negative Ha-Ras variant became tolerant to oxidative stress (3). Here, we have extended our analysis to tubular cells in vitro and kidney in vivo. We show that oxidative stress markedly induces Ras-ERK1/2. Inhibition of this cascade significantly reduced apoptosis. In vivo, this translates to a significant reduction of damage induced by transient ischemia using S-FTI. We suggest that farnesyl transferase inhibitors are the tools to achieve this protection in vivo.

MATERIALS AND METHODS

Cell cultures. Experiments were performed using semiconfluent human renal proximal tubular (HRPT) cells or human umbilical vein endothelial cells (ECV-304).

HRPT cells were cultured by using renal fragments of normal tissue (1–2 mm) obtained from kidneys excised in patients with renal cancer but with normal renal function and not affected by hepatitis viruses. The technique was described for the first time by Detrisac et al. (5): briefly, tubular cells were obtained through several passages in progressively narrowing filters, continuously washed, and subsequently treated with collagenase/dispase. Cells were cultured in DMEM-Ham's F-12 (Sigma, St. Louis, MO) enriched with insulin, transferrin, and selenite in 95% air-5% CO_2. The confluent cells were treated with trypsin and washed with Percoll solution. The specific isolation of proximal tubular cells was achieved by an immunomagnetic separation technique using monoclonal anti-human aminopeptidase M (AMP; CD13, Sigma), a specific marker of proximal tubular cells, as previously described (1). Flow-cytometric analysis showed that proximal tubular cells were positive for CD13 and negative for EMA, CD90, and von Will brand factor, specific markers of tubular distal cells, fibroblasts, and endothelial cells, respectively.

ECV-304 human endothelial cells (European Collection of Cell Cultures) were grown in monolayers in RPMI 1640 medium (Sigma) supplemented with 10% FBS (Sigma), 2 mM L-glutamine, 50 μg/ml streptomycin, and 50 IU/ml penicillin; the cells were kept in a 5% CO_2-95% air atmosphere at 37°C.

Flow cytometric analysis of cell death. Cell death was measured in HRPT cells using an annexin V detection kit (MBL Medical and Biological Laboratories, Watertown, MA). One week before the experiments, 1.25×10^5 cells were plated on 35-mm petri dishes and grown in complete medium. The cells were then collected by trypsinization and, after one wash in PBS, were suspended in 500 μl of binding buffer, stained with annexin V-FITC (an apoptosis marker) and propidium iodide (PI; a necrosis marker) and incubated at room temperature for 15 min before the flow cytometric analysis. Apoptotic (annexin V-FITC ^{pos}/PI^{neg}) and necrotic (annexin-V^{pos}/PI^{pos} and annexin-V^{neg}/PI^{pos}) cells were detected and quantified as a percentage of the entire population. To measure necrosis in ECV-304 cells, 1.4×10^5 cells were plated on 35-mm petri dishes and grown for 48 h in complete medium. After trypsinization and one wash in PBS, the cells were resuspended in 500 μl of PBS and 1 μg/ml of propidium iodide was added before the flow cytometric analysis of PI^{pos} cells.

Cytometric analysis was performed with a FACScan apparatus (Becton-Dickinson, San José, CA), and data were analyzed using WinMDI 2.8 software (J. Trotter, Scripps Research Institute, La Jolla, CA).

Immunoblot analysis. For immunoblot analysis of oxidative stress-induced Phospho-ERK1/2 and Phospho-Akt levels, renal tubular epithelial cells, grown to semiconfluence in 60-mm petri dishes, were incubated for 18 h in medium containing 0.2% FBS before H_2O_2 treatment. A sample growing in medium containing 10% FBS was used as control. Then, cells were harvested by scraping them into RIPA buffer (50 mM Tris·HCl, pH 7.5, 150 mM NaCl, 1% NP-40, 0.5% deoxycholate, 0.1% SDS) containing 2.5 mM Na-pyrophosphate, 1 mM β-glycerophosphate, 1 mM $NaVO_4$, 1 mM NaF, 0.5 mM PMSF, and a cocktail of protease inhibitors (Boehringer, Mannheim, Germany). Next, cell lysates were centrifuged for 10 min at 11,600 *g*, and the pellets were discarded. Fifty micrograms of protein were resolved by 10% SDS-PAGE and transferred onto polyvinylidene difluoride membranes. The membranes were then probed with monoclonal anti-phospho-ERK1/2 antibodies (Santa Cruz Biotechnology, Santa Cruz, CA) or with anti phospho-Akt antibodies (Cell Signaling, Beverly, MA) at 1:1,000 dilution, following the manufacturer's instructions. The membranes were then stripped and reprobed with antibodies at 1:1,000 dilution against polyclonal total ERK1/2 (Santa Cruz Biotechnology) and total Akt (Cell Signaling), respectively. Protein bands were revealed by enhanced chemiluminescence (Amersham Life Science).

For the immunoblot assay of membrane levels of prenylated proteins, cells grown to semiconfluence in 100-mm culture dishes in complete RPMI medium, were incubated for 18 h in the absence or in the presence of 1.8 μM S-FTI (Calbiochem, San Diego, CA), and then collected by scraping them into a buffer containing 100 mM KCl, 3 mM NaCl, 3.5 mM $MgCl_2$, 1.25 mM EGTA, 10 mM PIPES, 2 mM $NaVO_4$, 10 mM phenylarsine oxide, 5 mM NaF, and a cocktail of protease inhibitors. Cells were then disrupted by sonication (2- to 10-s pulses at 100 W) and centrifuged at 600 *g* for 10 min. Next, the supernatants were centrifuged at 100,000 *g* for 45 min. The membrane pellet was resuspended in a 50-μl RIPA buffer. Fifty micrograms of cytosol and membrane proteins were resolved by a 12% SDS-PAGE and transferred onto a polyvinylidene difluoride membrane. Next, the membrane was blocked in 3% nonfat dry milk in TBS-Tween 20 (0.05%) and probed with monoclonal anti-Pan-Ras (1:1,000, Upstate Biotechnology, Lake Placid, NY), anti-Ki-Ras (1:100, Santa Cruz Biotechnology), or polyclonal anti-Rab7 (H-50, 1:200, Santa Cruz Biotechnology) antibodies. Thus the membrane was washed and incubated with secondary horseradish-peroxidase-linked antibody (Amersham Pharmacia Biotech) (1:2,000), and the specific protein bands were detected by enhanced chemiluminescence and quantified by densitometry using Scion Image software.

For immunoblot analysis of kidney tissues, kidney fragments from rats in the acute hemodynamic studies (see below) were homogenized in 250 mM sucrose, 5 mM imidazole, pH 6.5, and 0.5 mM dithiothreitol (1:4, wt/vol), using a glass-Teflon potter. Samples were then centrifuged at 800 *g* at 4°C for 10 min, and supernatants were centrifuged at 100,000 *g* at 4°C for 45 min in a 70.1 Ti rotor (Beckman). Supernatants (cytosols) were collected, and membrane pellets were suspended in RIPA buffer. Fifty micrograms of membrane and cytosolic fractions were then subjected to immunoblot analysis for Pan-Ras and Ki-Ras proteins, following the procedure described above.

Determination of protein content. Protein content of total lysates and of membrane and cytosolic fractions was determined according to the method of Lowry (11).

Animal studies. This study was carried out in 44 male Sprague-Dawley rats (3 mo old, Charles River) fed a standard diet (19% protein content as casein) and tap water ad libitum. The experimental protocol and surgical procedures using animals were carried out according to Italian law and were approved by Italian Ministry of Health.

Downloaded from journals.physiology.org/journal/ajprenal (092.021.147.200) on April 1, 2022.

After light anesthesia with pentobarbital sodium (Nembutal, 50 mg/kg ip), the right kidney was nephrectomized under sterile conditions. Seven days later, the rats were randomly assigned to one of the following groups: IRI, untreated rats with acute renal ischemia ($n = 8$); S-FTI, rats with IRI pretreated with S-FTI (Biomol Research Lab, $n = 10$); and NOR, sham-operated rats ($n = 9$).

Ischemic damage was induced by clamping the left renal artery for 45 min with an atraumatic vascular clamp under anesthesia (Nembutal, 50 mg/kg ip). The reperfusion of the kidney was confirmed visually before suturing of the abdominal wall. The sham operation consisted of the same surgical procedure except that the renal artery was not closed. All the rats were treated 4 h before this procedure either with S-FTI (0.26 μg/kg body wt ip, dissolved in 0.3 ml of saline solution; S-FTI group) or with saline solution in equivalent volumes (IRI and NOR groups). The rats were then restrained, and 24 h later were surgically prepared for a hemodynamic study under Inactin anesthesia (100 mg/kg ip). All surgical procedures were carried out on an automatically thermo-regulated table, which maintained the rat's constant body temperature (37.5°C), as assessed by a rectal probe connected to a thermometer.

The details of surgical procedures are described elsewhere (18, 19). After a 60-min stabilization period, three to five clearance periods were performed in each experiment for the collection of blood samples from the femoral artery and renal vein (through a sharpened glass micropipettes), to assess the arteriovenous gradient of inulin, an estimate of the renal filtration fraction.

At the end of the experiment, the kidney was carefully removed and weighed under sterile conditions, and samples of renal tissue were immediately stored (−80°C) for the evaluation of Ras protein activation.

The dosage of S-FTI was carefully established in four groups of rats ($n = 4$/group), with a wide range of doses (0.16–1.3 μg/kg); the dose we used was associated with the best functional and histological outcome.

In an additional group of animals ($n = 3$), the ability of S-FTI in mitigating renal damage after induction of IRI was tested by the intravenous administration of the drug 1 h after reperfusion. During the clamping of the renal artery, the right femoral vein was isolated and catheterized (PE-50 tubing), and S-FTI (0.15 μg/kg body wt in 0.2 ml of saline solution) was injected 60 min after clamp removal. This policy was adopted to avoid altered peritoneal absorption of the drug when the abdomen was open and the rat was still anesthetized; lower doses of the drug were used. Also in this case, the reported dosage fit the best functional outcome. Control rats ($n = 3$) were treated with 0.2 ml of saline solution.

Analytic determinations. Urinary volume was measured gravimetrically in preweighed vials. The concentrations of inulin in plasma and urine were measured by the diphenylamine method. The urine for determination of urinary nitrate concentration was collected in sterile vials under ice (4°C), filtered through a 0.2-μm filter (Acrodisc, Gelman), and frozen until the time of assay (−80°C). The dosage was carried out by a total nitric oxide assay utilizing nitrate reductase and the Griess reagent (RD Systems). Proteinuria was determined by the Bio-Rad method, according to the manufacturer's instructions.

The filtration fraction was measured by renal extraction of inulin [arterial − venous/arterial concentration (A − V/A) × 100]; renal plasma flow (RPF) was calculated by the ratio glomerular filtration rate (GFR)/filtration fraction (FF), and renal blood flow by correction of RPF by hematocrit [RBF = RPF/(1 − Hct)/100]; renal vascular resistances (RVR) were estimated by the expression RVR = MAP/RBF, where MAP represents the mean arterial pressure.

Histology. Specimens of renal parenchyma were fixed in activated Bouin's solution for histological examination, and plastic-embedded 3-μm sections were cut, stained with hematoxylin-eosin, periodic acid-Schiff, Jones staining, and observed in a blinded fashion. Fifty proximal tubules from the outer stripe of the outer medulla (OSOM) were examined in each rat at ×400 magnification and assigned to three categories: tubules with normal appearance (0); tubules with signs of moderate to sublethal injury (loss of apical brush border; 1); tubules with signs of acute tubular necrosis (from a few sloughed epithelial cells to tubules with a complete naked basal membrane; 2). Proximal tubules were distinguished from distal tubules on the basis of morphological criteria (18).

Statistics. The ANOVA was used to compare the different mean values in the different groups of rats. Bonferroni's test was used to find significant differences among the groups under study. Histological data were analyzed by the Kruskal-Wallis ANOVA followed by Dunn's multiple comparison test. A P value <0.05 was considered statistically significant. The data are expressed as means ± SD. Statistical differences in cell experiments were evaluated using a Student's t-test for unpaired samples.

RESULTS

Ras/ERK1/2 activation promotes oxidative stress-induced cell death in HRPT cells. HRPT cells exposed to increasing concentrations of H_2O_2 activated stress kinases and a variety of signaling proteins, including some mediators of apoptosis. High H_2O_2 concentrations and longer periods of treatment induced cell death, which was monitored by FACS analysis. Figure 1, *A* and *B*, shows that H_2O_2 for 18 h essentially induced necrosis in a dose-dependent manner and apoptosis in a smaller fraction of cells; shorter periods of exposure to H_2O_2 (6 h) or lower concentrations reduced the fraction of necrotic cells and increased apoptosis (data not shown). Oxidative stress by 1 mM H_2O_2 robustly induced ERK1/2 and Akt, two important downstream targets of Ras, with a peak at 2 min for ERK1/2 and 30 min for Akt (Fig. 1*C*). The activation of these kinases preceded the onset of cell death, detectable 3 h after treatment (data not shown).

The ERK1/2 cascade is activated essentially by Ras-Raf1-MEK signaling (28). To test the role of both MEK-ERK1/2 and Akt in H_2O_2-induced cell death, we inhibited ERK1/2 activation by pretreating tubular cells with 40 μM PD-98059 (Calbiochem), a specific inhibitor of MEK1. We also prevented Akt activation by treating the cells with LY-294002 (Calbiochem), a specific inhibitor of PI3-kinase, the upstream activator of Akt. Figure 1*D* shows that the fraction of cells undergoing apoptosis and necrosis was significantly reduced by PD-98059 compared with untreated cells; conversely, LY-294002, the PI3-kinase inhibitor, did not significantly affect stress-induced cell death. We note that the fraction of cells protected by PD-98059 treatment was significantly reduced in the control, although the relative rate of apoptosis was increased. Because the fraction of cells undergoing apoptosis was rather small (3%), the protective effects of PD-98059 were better appreciated in a larger population of cells undergoing necrosis.

Because ERK1/2 is activated by Ras, we inhibited Ras by using S-FTI, which selectively alters its membrane binding, necessary for its biological activity. To determine the specificity of action of S-FTI, we measured the fraction of Ras in membranes of HRPT cells incubated with 1.8 μM S-FTI for 18 h. Figure 2*A* shows that S-FTI treatment consistently reduced membrane-bound Ras (−34 ± 3%) and increased the cytosolic fraction. Under these conditions, S-FTI inhibited H_2O_2-dependent activation of ERK1/2 (Fig. 2*B*). Thus HRPT cells were incubated for 18 h in the presence and absence of 1.8 μM S-FTI in medium containing 0.2% FBS to downregulate phospho-ERK1/2 levels. The cells were then stimulated with 1 mM H_2O_2 for 2 and 30 min, and phospho-ERK1/2 and total

Downloaded from journals.physiology.org/journal/ajprenal (092.021.147.200) on April 1, 2022.

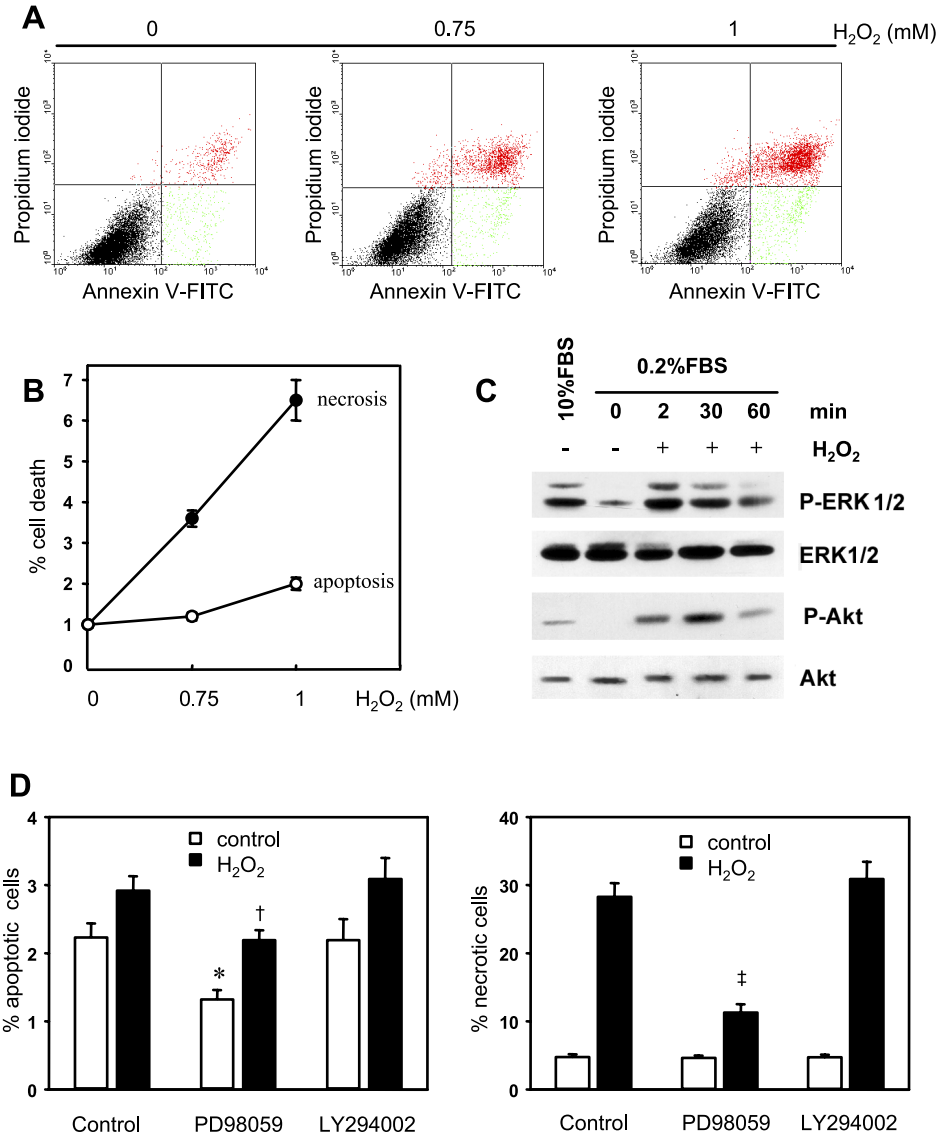

Fig. 1. ERK1/2 inhibition prevents human renal proximal tubular (HRPT) cells from oxidative-stress-induced cell death. *A*: flow cytometric analysis of cell death in HRPT cells treated for 18 h with the indicated concentrations of H_2O_2. The cells were collected by trypsinization and double stained with annexin V-FITC (apoptosis marker) and propidium iodide (necrosis marker). Annexin-V^{neg}/PI^{pos} and annexin-V^{pos}/PI^{pos} (*top left* and *top right*, red) events represent necrotic cells; annexin-V^{pos}/PI^{neg} (*bottom right*, green) events represent apoptotic cells. The figure shows the dot plots of a representative experiment. *B*: fold-induction of the percentages of apoptotic and necrotic cells on total cell population following oxidative stress with increasing concentrations of H_2O_2 measured as described in *A*. Values are means ± SD of 3 independent experiments performed in duplicate. *C*: time course of ERK1/2 and PI3-K activation in HRPT cells following oxidative stress. The cells were incubated for 18 h in medium containing 0.2% FBS, treated for the indicated time intervals with 1 mM H_2O_2, and then analyzed by Western blotting using antibodies against the phosphorylated form of ERK1/2 and of Akt. The 1st lane was loaded with a sample growing in 10% FBS. To normalize for sample loading and protein transfer, the same membranes were stripped and reprobed with antibodies against total ERK1/2 and total Akt, respectively. Representative results from 1 of 3 experiments are shown. *D*: flow cytometric analysis of H_2O_2-induced cell death in HRPT cells treated with ERK1/2 and phosphoinositide 3-kinase (PI3-kinase) inhibitors. Cells were treated for 30 min with 40 μM PD-98059 (ERK1/2 inhibitor) or for 15 min with 50 μM LY-294002 (PI3-kinase inhibitor) and then for 18 h with 0.75 mM H_2O_2 in the presence of the inhibitors. Apoptosis and necrosis were evaluated as in *A*. Controls were treated with vehicle (DMSO). Values (means ± SD, $n = 3$) are the percentages of apoptotic and necrotic cells on total cell population. *$P < 0.05$ vs. unstressed control. †$P < 0.01$ vs. H_2O_2-treated control. ‡$P < 0.001$ vs. H_2O_2-treated control.

ERK1/2 levels were measured. Figure 2*B* shows that treatment with S-FTI markedly reduced H_2O_2-induced P-ERK1/2 levels, thus confirming the ability of this inhibitor to downregulate the Ras/ERK1/2 pathway. S-FTI treatment, in the same condition, was also able to inhibit ERK1/2 activation induced by stimulation of the cells for 2–5 min with 20% FBS (data not shown).

To determine the effects of this pathway on oxidative-induced cell death, we stressed the cells with H_2O_2 for 18 h in the presence of S-FTI. The drug significantly reduced the levels of apoptotic and necrotic cells in stressed samples compared with untreated cells, without affecting basal levels of cell death (Fig. 2*C*). To exclude that the protective effects of S-FTI and PD-98059 against oxidative stress-dependent injury are mediated by a chemical antioxidant activity of these substances, we measured by a spectrophotometric in vitro assay (8) their ability to convert the green-blue 2,2′-azino-bis(3-ethylbenzthiazoline-6-sulfonic acid), $ABTS^{\cdot+}$ radical, to the uncolored ABTS cation; both substances failed to reduce the $ABTS^{\cdot+}$ radical levels, thus demonstrating that they do not possess antioxidant activity (data not shown).

Endothelial cells represent an important cellular fraction of the kidney and are potential targets of oxidative stress injury. In human umbilical vein endothelial cells, oxidative stress determines activation of the ERK1/2 pathway and cell death; the inhibition of farnesylprotein transferase in these cells reduces H_2O_2-induced ERK1/2 phosphorylation (3). Therefore, we have studied the effects of S-FTI on survival of stabilized endothelial cells (ECV-304) subjected to oxidative stress. Because ECV-304 cells are more sensitive to oxidative stress than HRPT cells, we treated them for 18 h with a lower dose (500 μM) of H_2O_2. S-FTI exerted a significant protective effect on H_2O_2-induced cell death (Fig. 3*A*), and Ras displacement from cell membrane after S-FTI treatment was also confirmed in ECV-304 cells (Fig. 3*B*). Ki-Ras localization was not influenced by S-FTI treatment (Fig. 3*B*), because this isoform is also geranylated (9). These data indicate that Ha-Ras is the principal Ras isoform affected by S-FTI treatment. Moreover, membrane localization of another farnesylated protein, Rab7, bound to late endosome and not permanently resident in the plasma mem-

Downloaded from journals.physiology.org/journal/ajprenal (092.021.147.200) on April 1, 2022.

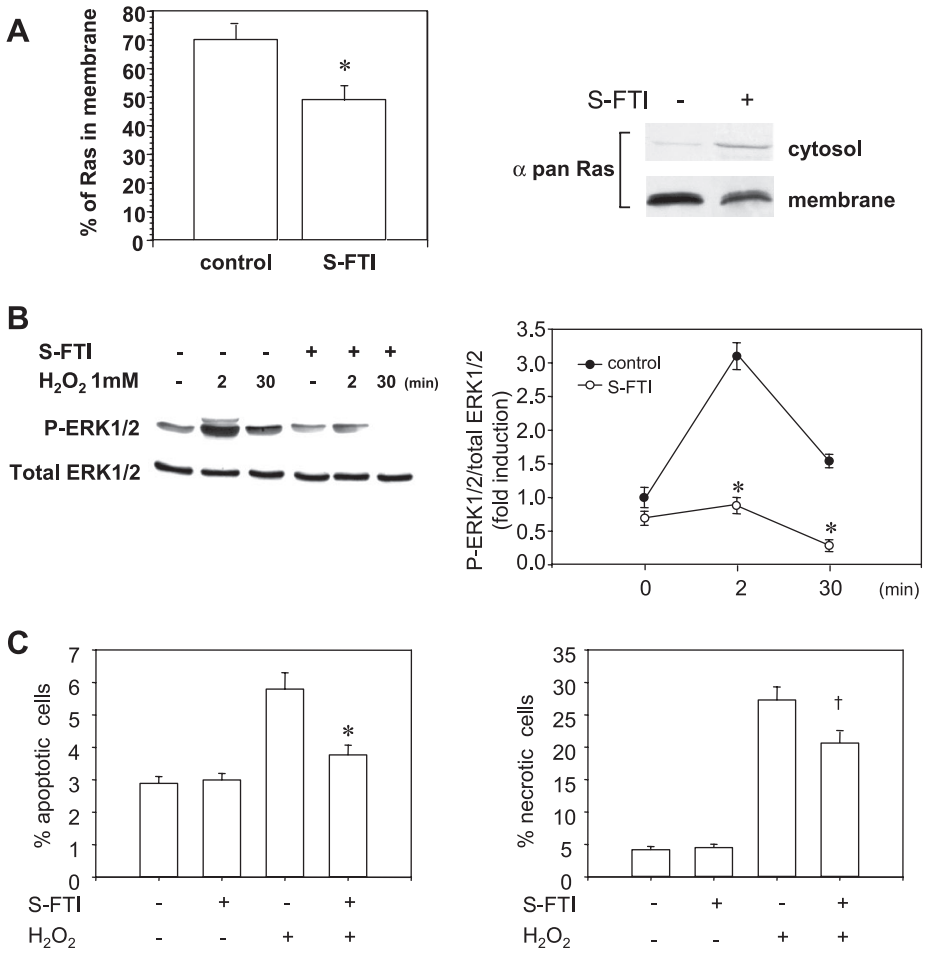

Fig. 2. Chaetomellic acid A (S-FTI) inhibits Ras/ERK1/2 pathway and protects HRPT cells from oxidative stress-induced cell death. *A*: S-FTI displaces Ras protein from the membrane. HRPT cells were treated with 1.8 μM S-FTI for 18 h, and then 50 μg of membrane and cytosolic fractions were subjected to immunoblotting with anti-Ras antibodies (*right*). The protein bands were quantified by densitometric analysis. *Left*: histograms show the percentages (means ± SD, $n = 3$) of the Ras protein in membrane with respect to the total (cytosol+membrane). *$P < 0.05$ vs. control. *B*: S-FTI inhibits H_2O_2-dependent ERK1/2 activation. *Left*: cells were starved in medium containing 0.2% FBS for 18 h in the absence and presence of 1.8 μM S-FTI and then stimulated with 1 mM H_2O_2 for the indicated time intervals. Fifty micrograms of total cell lysates were subjected to immunoblotting using antibodies against the phosphorylated (active) form of ERK1/2. The same filters were stripped and reprobed with antibodies against total ERK1/2 and both phospho and total ERK1/2 bands, revealed by enhanced chemiluminescence, were subjected to densitometric analysis. Shown is a representative immunoblot experiment. *Right*: phospho ERK1/2 values were normalized for total ERK1/2 values and plotted as fold-induction compared with control, not stimulated sample. Values are means ± SD of 3 independent experiments. *$P < 0.001$ vs. controls. *C*: S-FTI protects HRPT cells from H_2O_2-induced oxidative stress. Cells were treated for 5 h with 1.8 μM S-FTI and then for 18 h with 1 mM H_2O_2 in the presence of S-FTI. Apoptosis and necrosis were analyzed as in Fig. 1*A*. Values shown in the histogram (means ± SD, $n = 3$) are the percentages of apoptotic or necrotic cells in total cell population. *$P < 0.005$ vs. H_2O_2-treated control. †$P < 0.05$ vs. H_2O_2-treated control.

brane (27), was not affected by S-FTI treatment in ECV cells (Fig. 3*B*).

Pretreatment with S-FTI attenuates postischemic injury in the rat. To translate the above-mentioned data in vivo, we used a specific model of acute IRI in the uninephrectomized rat. Briefly, the renal artery was transiently occluded (45 min), and 24 h after the ischemia renal injury was assessed by hemodynamic and biochemical studies. The data from the hemodynamic analysis are reported in Table 1. There was no change in body weight and hematocrit values among the three groups of rats under observation. GFR averaged 0.9 ± 0.4 ml·min^{-1}·100 g body wt^{-1} in normal rats (NOR group) and was significantly depressed in IRI rats (0.17 ± 0.1 ml·min^{-1}·100 g body wt^{-1}; −81.1%, $P < 0.001$ vs. NOR group). Pretreatment with S-FTI determined a consistently better preservation of renal function after ischemia (GFR, 0.50 ± 0.1 ml·min^{-1}·100 g body wt^{-1}), significantly higher compared with the IRI group ($P < 0.05$). The filtration fraction, measured as the arteriovenous gradient of inulin, averaged 26.5 ± 3.4% in normal rats and was significantly depressed in rats in the S-FTI group (−23.3% vs. NOR, $P < 0.001$, Student's *t*-test). It is worth pointing out that we were not able to measure the arteriovenous gradient of inulin in five of eight rats from the IRI group, due to the massive functional and histological damage induced by ischemia-reperfusion (see below). This precluded the calculation of the parameters regulating renal dynamics in this group. In S-FTI rats, the decrease in GFR was caused by increased renal vascular resistances (+42.9%, $P < 0.001$), and the consequent reduction of renal blood flow, compared with rats in the NOR group. Nitrate excretion was significantly decreased in IRI rats (−71% vs. NOR, $P < 0.05$); similarly, pretreatment with S-FTI completely prevented the fall in nitrate excretion (−19% vs. NOR, $P < 0.05$ vs. IRI).

Displacement of Ras from cell membrane by S-FTI in whole kidney. Sections of kidneys derived from rats undergoing the hemodynamic study were homogenized, and membrane and cytosolic fractions were subjected to immunoblotting with anti-Pan-Ras and anti Ki-Ras antibodies, as described in MATERIALS AND METHODS.

Figure 4 shows that pretreatment with S-FTI determined a significant decrease in membrane-bound Ras proteins (−55%) without affecting Ki-Ras membrane binding, in agreement with the results obtained in cells.

Pretreatment with S-FTI attenuates histological damage in acute postischemic injury in the rat. Figure 5 shows that nearly 85% of the proximal tubular segments in OSOM appeared normal in control rats (NOR group). The ischemic insult determined a significant necrosis in rats of the IRI group (averaging 30%), and signs of injury were present in almost all of the cells. Pretreatment with S-FTI virtually prevented cellular necrosis and reduced the number of injured cells. Our analysis indicated that approximately one-half the fraction of tubular cells did not show signs of injury (S-FTI group).

Downloaded from journals.physiology.org/journal/ajprenal (092.021.147.200) on April 1, 2022.

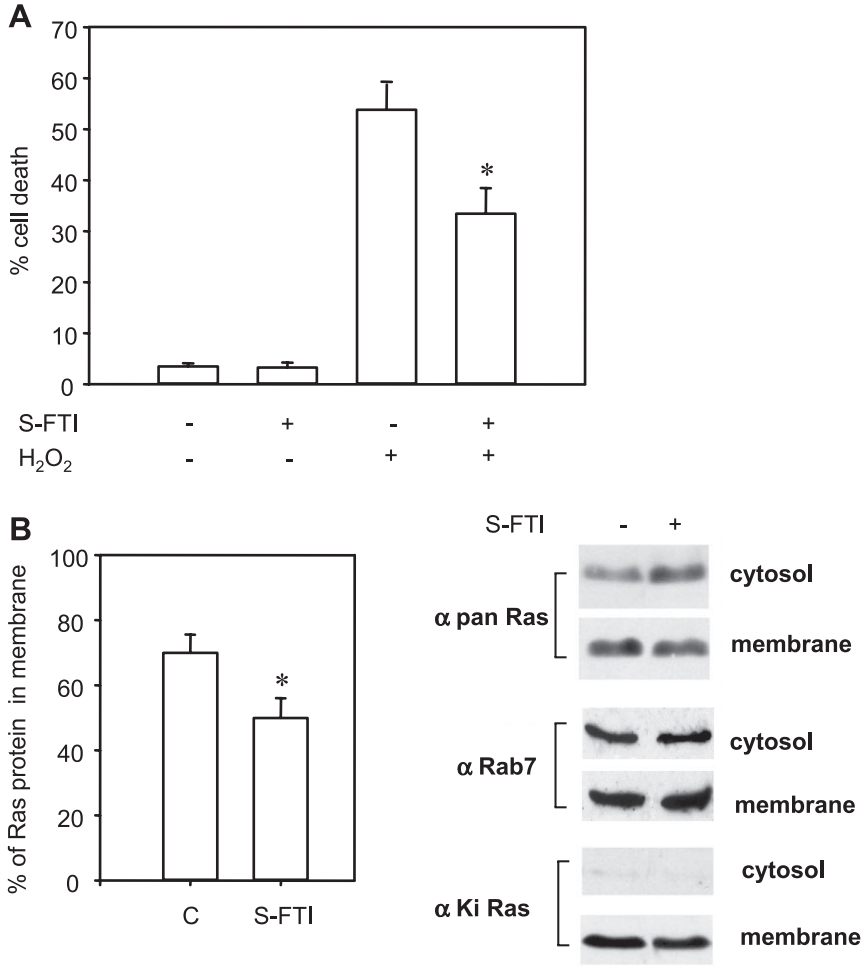

Fig. 3. Effects of S-FTI on endothelial ECV-304 cells. *A*: S-FTI protects ECV-304 cells from H_2O_2-induced cell death. Cells were treated for 5 h with 1.8 μM S-FTI and then for 18 h with 500 μM H_2O_2 in the presence of S-FTI. The cells were collected by trypsinization, stained with propidium iodide, and analyzed by flow cytometry. Values are means ± SD of 3 independent experiments. $*P < 0.05$ vs. H_2O_2-treated control. *B*: S-FTI displaces Pan-Ras, but not Ki-Ras or Rab7 proteins from the membrane of ECV-304 cells. Cells were treated with 1.8 μM S-FTI for 18 h, and then 50 μg of membrane and cytosolic fractions of control (C) and treated samples were subjected to immunoblotting with the specific antibodies and the protein bands were quantified by densitometric analysis. The histogram shows the percentages (means ± SE, $n = 3$) of Pan-Ras in membrane with respect to the total amount present in the cytosol and membrane. $*P < 0.05$ vs. control.

Effects of the administration of S-FTI after ischemia-reperfusion injury in the rat. In three additional rats, S-FTI was administered intravenously 1 h after IRI and renal dynamics were evaluated 24 h later. Also, these rats evidenced a beneficial effect after S-FTI treatment, because their GFR averaged 0.456 ± 0.11 $ml \cdot min^{-1} \cdot 100\ g\ body\ wt^{-1}$. In control rats of this group ($n = 3$), GFR values overlapped those of rats in the IRI group.

DISCUSSION

Our study demonstrates that pretreatment with S-FTI of tubular and endothelial cells subjected to an oxidative stress significantly reduced apoptosis. S-FTI dislodged Ha-Ras from cellular membranes and reduced ERK1/2 activation. Similar effects were obtained in vivo in rats: the animals treated with this compound were selectively protected by the acute renal damage induced by ischemia.

In recent years, apoptosis and inflammation have been proposed as potential targets to limit organ damage after an ischemic insult (2, 4), and Ras seems to play a crucial role in mediating both phenomena. We have previously found that activation of Ha-Ras substantially increased apoptosis induced by oxidative stress in endothelial cells (3) and that Ha-Ras selectively stimulated NADPH oxidase and increased ROS

Table 1. *Renal hemodynamics and urinary nitrate excretion in the different groups under study*

	BW, g	KW, g	BP, mmHg	Ht, %	GFR, $ml \cdot min^{-1} \cdot 100\ g\ BW^{-1}$	FF, %	RPF, $ml \cdot min^{-1} \cdot 100\ g\ BW^{-1}$	RBF, $ml \cdot min^{-1} \cdot 100\ g\ BW^{-1}$	RVR, $mmHg \cdot ml^{-1} \cdot min$	NITR, $nmol \cdot min^{-1} \cdot g\ KW$
NOR ($n = 9$)	319.7±42.3	1.541±0.1	114±10	44.0±2.0	0.90±0.4	26.5±3.4	3.37±1.2	5.97±2.1	19.53±9.1	8.24±3.7
IRI ($n = 8$)	296.2±19.6	1.690±0.3	113±10.7	43.2±2.4	0.17*± 0.1	NA	NA	NA	NA	2.39‡±0.9
S-FTI ($n = 10$)	319.0±37.7	1.753±0.3	119±4.8	42.0±1.7	0.50†±0.1	20.3§±2.2	2.48§±0.6	4.29§±1.3	27.91§±6.9	6.63±1.7

Values are means ± SD. *n,* No. of rats. Nitrate excretion was determined only in 7, 7, and 8 rats in the sham operated (NOR) ischemia-reperfusion injury (IRI) and chaetomellic acid A (S-FTI) group, respectively. BW, body weight; KW, kidney weight; BP, mean blood pressure; Ht, hematocrit; GFR, glomerular filtration rate factored for BW; FF, filtration fraction; RPF, renal plasma flow; RBF, renal blood flow; RVR, renal vascular resistance; NITR, urinary nitrate excretion; NA, data not available. $*P < 0.001$ vs. NOR. †$P < 0.01$ vs. NOR and $P < 0.05$ vs. IRI (ANOVA and Bonferroni correction). ‡$P < 0.01$ vs. NOR and $P < 0.05$ vs. S-FTI (ANOVA). §$P < 0.05$ vs. NOR (minimum value, Student's *t*-test for unpaired data between S-FTI and NOR groups.

Downloaded from journals.physiology.org/journal/ajprenal (092.021.147.200) on April 1, 2022.

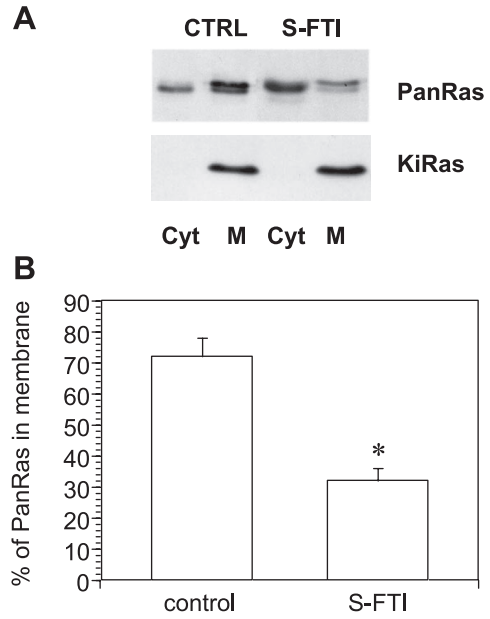

Fig. 4. Treatment of rats with S-FTI causes the displacement of Ras protein from the membrane of kidney tissues. Fifty micrograms of cytosolic and membrane fraction proteins from kidney of ischemia-reperfusion injury (IRI) and S-FTI-treated animals were subjected to immunoblotting with anti-pan-Ras or anti-Ki-Ras antibodies. *A*: Pan-Ras and Ki-Ras protein bands of cytosol (Cyt) and membrane (M) fractions of a representative control (CTRL) and S-FTI-treated animal. *B*: histogram shows the percentages (means ± SD, $n = 6$) of Pan-Ras protein in membrane with respect to the total (cytosol+membrane). *$P < 0.001$ vs. control.

production (20, 22), whereas cells expressing Ki-Ras, which stimulated mitochondrial SOD, were resistant to the same type of stress (20). Moreover, we and others have provided evidence that farnesyl transferase inhibitors dislodge and inactivate Ha-Ras and do not influence membrane localization of Ki-Ras (Fig. 3*B*) (3, 9).

The data presented here provide further insights into the mechanism underlying renal damage induced by ischemia. These observations suggest the following mechanism: endothelial and tubular cells, subjected to oxidative stress, activate stress kinases, including Ras/ERK1/2. This circuitry amplifies the effects of Ras and ERK1/2 on membrane NADPH oxidase (22). Inhibition of Ha-Ras by S-FTI downregulates this loop and significantly reduces apoptosis elicited by transient ischemia. Compared with other inhibitors, the action of S-FTI appears rather selective. Rab 7, for example, located in the inner membranes, or Ki-Ras, localized on the plasma membrane with two lipid anchors, are not altered.

An attractive result of our study is the translation of cellular findings to the whole animal: the displacement of Ras from cell membrane by S-FTI represents the first demonstration in vivo that parallels the significant reduction of ischemic organ damage by S-FTI. The demonstration of an arteriovenous gradient for inulin in all the S-FTI rats, contrary to the untreated ischemic rats (the IRI group), is a further positive effect that reflects either the higher GFR or the decreased "backfiltration" of inulin through the damaged tubules, commonly occurring after a prolonged ischemia. Histological data are in agreement with these results, showing the total disappearance of cellular necrosis in rats treated with S-FTI, with a considerable number of completely normal cells.

Although we cannot precisely identify the cells carrying activated Ras in the organ, we believe that tubular, endothelial, and mesenchymal cells contain stabilized Ha-Ras. We have recently provided evidence that normal fibroblasts and human primary cells regulate Ras levels by proteasomal degradation. H_2O_2 or ROS in vitro and in vivo increase and activate Ha-Ras (23). We have recently extended these observations to rat ischemic neurons, mouse astrocytes, and peripheral human lymphocytes (Avvedimento VE and Santillo M, unpublished observations). Stabilized and immortalized cell clones lose this regulation and modulate Ras activity solely by GTP-GDP binding.

The data presented here describe the protective effects of a farnesyl transferase inhibitor on ischemic renal cell injury in isolated tubular and endothelial cells and in whole kidney.

The results of this study have a broader impact, because they indicate a pharmacological tool for reducing ischemic damage in vivo. For example, kidneys to be transplanted can be better preserved and significantly reduce the extent of the damage if pretreated with S-FTI. Moreover, the possibility that S-FTI may be beneficial even when the drug is administered after the ischemic insult opens new, intriguing perspectives in the treatment of IRI, although conclusive evidence awaits the response of a larger number of animals.

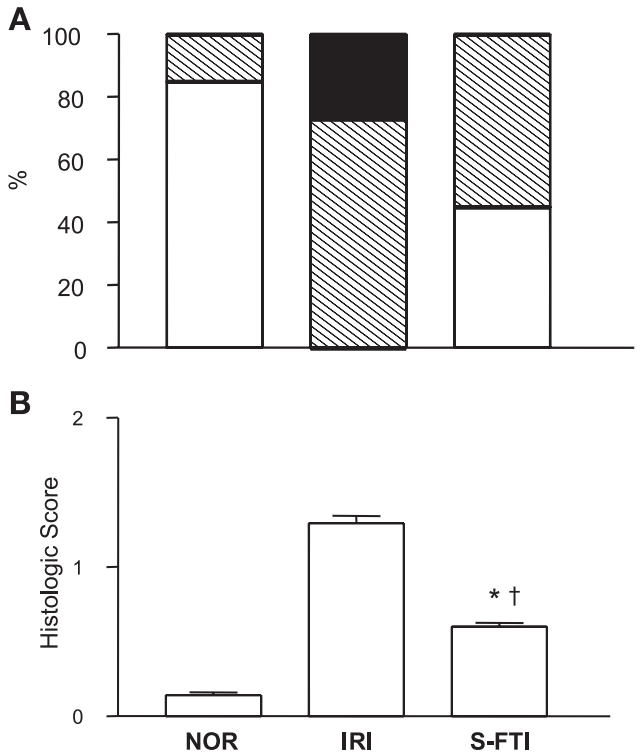

Fig. 5. Histological evaluation of renal tubular damage after ischemia. *Top*: percentages of proximal tubules in the outer stripe of the outer medullar (OSOM) categorized as tubules with a normal appearance (open portion), tubules with signs of sublethal injury (dashed lines portion), and tubules with signs of acute tubular necrosis (filled portion). *Bottom*: tubules with a normal appearance, tubules with signs of sublethal injury, and tubules with signs of acute tubular necrosis were scored 0, 1, and 2, respectively. Columns represent the mean score (±SE). NOR, sham-operated rats. *$P < 0.05$ vs. NOR. †$P < 0.05$ vs. NOR.

Downloaded from journals.physiology.org/journal/ajprenal (092.021.147.200) on April 1, 2022.

GRANTS

This work was partly supported by the Italian Association for Cancer Research and the Italian Ministry of University and Scientific Research (Cofin 2002, Grant 065485).

REFERENCES

1. **Baer PC, Nockher WA, Haase W, and Scherberich JE.** Isolation of proximal and distal tubule cells from human kidney by immunomagnetic separation. *Kidney Int* 52: 1321–1331, 1997.
2. **Bonventre JV and Zuk A.** Ischemic acute renal failure: an inflammatory disease? *Kidney Int* 66: 480–485, 2004.
3. **Cuda G, Paternò R, Ceravolo R, Candigliota M, Perrotti N, Perticone F, Faniello MC, Schepis F, Ruocco A, Mele E, Cassano S, Bifulco M, Santillo M, and Avvedimento EV.** Protection of human endothelial cells from oxidative stress. Role of Ras-ERK1/2 signalling. *Circulation* 105: 968–974, 2002.
4. **Daemen MA, van't Veer C, Denecker G, Heemskerk VH, Wolfs TG, Clauss M, Vandenabeele P, and Buurman WA.** Inhibition of apoptosis induced by ischemia-reperfusion prevents inflammation. *J Clin Invest* 104: 541–549, 1999.
5. **Detrisac CJ, Sens MA, Garvin AJ, Spicer SS, and Sens DA.** Tissue culture of human kidney epithelial cells of proximal tubule origin. *Kidney Int* 25: 383–390, 1984.
6. **Doi K, Suzuki Y, Nakao A, Fujita T, and Noiri E.** Radical scavenger edaravone developed for clinical use ameliorates ischemia/reperfusion injury in rat kidney. *Kidney Int* 65: 1714–1723, 2004.
7. **Du Bose TD Jr, Warnock DG, Meht RL, Bonventre JV, Hammerman MR, Molitoris BA, Paller MS, Siegel NJ, Scherbenske J, and Striker GE.** Acute renal failure in the 21st century: recommendations for management and outcomes assessment. *Am J Kidney Dis* 29: 793–799, 1998.
8. **Fischer MA, Gransier TJ, Beckers LM, Bekers O, Bast A, and Haenen GR.** Determination of the antioxidant capacity in blood. *Clin Chem Lab Med* 43: 735–740, 2005.
9. **James GL, Goldstein JL, and Brown MS.** Polylysine and CVIM sequences of K-RasB dictate specificity of prenylation and confer resistance to benzodiazepine peptidomimetic in vitro. *J Biol Chem* 270: 6221–6226, 1995.
10. **Kelly KJ, Plotkin Z, and Dagher PC.** Guanosine supplementation reduces apoptosis and protects renal function in the setting of ischemic injury. *J Clin Invest* 108: 1291–1298, 2001.
11. **Lowry OH, Rosbrough NJ, Farr AL, and Randall RJ.** Protein measurement with the Folin-phenol reagents. *J Biol Chem* 193: 265–275, 1951.
12. **Lu CY, Penfield JG, Kielar ML, Vasquez MA, and Jeyarajah DR.** Hypothesis: is renal allograft rejection initiated by the response to injury during the transplant process? *Kidney Int* 55: 2157–2168, 1999.
13. **Magee T and Marshall C.** New insights into the interaction of Ras with the plasma membrane. *Cell* 98: 9–12, 1999.
14. **Marshall CJ.** Ras effectors. *Curr Opin Cell Biol* 8: 197–204, 1996.
15. **Matsumoto M, Makino Y, Tanaka T, Tanaka H, Ishikaza H, Noiri E, Fujita T, and Nangaku M.** Induction of renoprotective gene expression by cobalt ameliorates ischemic injury of the kidney in rats. *J Am Soc Nephrol* 14: 1825–1832, 2003.
16. **Ojo AO, Wolfe RA, Held PJ, Port FK, and Schmouder RL.** Delayed graft function: risk factors and implications for renal allograft survival. *Transplantation* 63: 1620–1628, 1997.
17. **Paller MS, Hoidal JR, and Ferris TF.** Oxygen free radicals in ischemic acute renal failure in the rat *J. Clin Invest* 74: 1156–1164, 1984.
18. **Sabbatini M, Pisani A, Uccello F, Serio V, Serù R, Paternò R, Cianciaruso B, Fuiano G, and Andreucci M.** Atorvastatin improves the course of ischemic acute renal failure in aging rats. *J Am Soc Nephrol* 15: 901–909, 2004.
19. **Sabbatini M, Sansone G, Uccello F, De Nicola L, Giliberti A, Sepe V, Magri P, Conte G, and Andreucci VE.** Functional versus structural changes in the pathophysiology of acute ischemic renal failure in aging rats. *Kidney Int* 45: 1355–1361, 1994.
20. **Santillo M, Mondola P, Serù R, Annella T, Cassano S, Ciullo I, Tecce MF, Iacomino G, Damiano S, Cuda G, Paternò R, Martignetti V, Mele E, Feliciello A, and Avvedimento EV.** Opposing functions of Ki- and Ha-Ra genes in the regulation of redox signals. *Curr Biol* 11: 614–619, 2001.
21. **Sebti SM and Adjei AA.** Farnesyltransferase inhibitors. *Semin Oncol* 29: 3–39, 2004.
22. **Serù R, Mondola P, Damiano S, Svegliati S, Agnese S, Avvedimento EV, and Santillo M.** HaRas activates the NADPH oxidase complex in human neuroblastoma cells via extracellular signal-regulated kinase 1/2 pathway. *J Neurochem* 91: 613–622, 2004.
23. **Svegliati S, Cancello R, Sambo P, Luchetti M, Paroncini P, Orlandini G, Discepoli G, Paterno R, Santillo M, Cuozzo C, Cassano S, Avvedimento EV, and Gabrielli A.** Platelet-derived growth factor and reactive oxygen species (ROS) regulate Ras protein levels in primary human fibroblasts via ERK1/2. Amplification of ROS and Ras in systemic sclerosis fibroblasts. *J Biol Chem* 280: 36474–36482.
24. **Thadhani R, Pacual M, and Bonventre JV.** Acute renal failure. *N Engl J Med* 334: 1448–1460, 1996.
25. **Thiemermann C, Patel NSA, Kvale EO, Cockerill GW, Brown PAJ, Stewart KN, Cuzzocrea S, Britti D, Mota-Filipe H, and Chatterjee PK.** High density lipoprotein (HDL) reduces renal ischemia/reperfusion injury. *J Am Soc Nephrol* 14: 1833–1843, 2003.
26. **Torras J, Cruzado JM, Riera M, Condom E, Duque Herrero I, Merlos M, Espinosa L, Lloberas N, Egido J, and Grinyo JM.** Long-term-protective effect of UR-12670 after warm renal ischemia in uninephrectomized rats. *Kidney Int* 56: 1798–1808, 1999.
27. **Vitelli R, Santillo M, Lattero D, Chiariello M, Bifulco M, Bruni CB, and Bucci C.** Role of the small GTPase Rab7 in the late endocytic pathway. *J Biol Chem* 272: 4391–4397, 1997.
28. **Waskiewicz AJ and Cooper JA.** Mitogen and stress response pathways: MAP kinase cascades and phosphatase regulation in mammals and yeast. *Curr Opin Cell Biol* 7: 798–805, 1995.

Downloaded from journals.physiology.org/journal/ajprenal (092.021.147.200) on April 1, 2022.